Molecular Biology of the Cell
Vol. 6, 559–576, May 1995

Loss of Cell Surface Syndecan-1 Causes Epithelia to Transform into Anchorage-independent Mesenchyme-like Cells

Masato Kato, Scott Saunders, Hung Nguyen,* and Merton Bernfield†

Joint Program in Neonatology, Harvard Medical School, Boston, Massachusetts 02115

Submitted November 4, 1994; Accepted March 13, 1995
Monitoring Editor: Masatoshi Takeichi

Simple epithelial cells are polygonal in shape, polarized in an apical-basal orientation, and organized into closely adherent sheets, characteristics that result from a variety of cellular specializations and adhesive proteins. These characteristics are lost when the epithelia transform during embryogenesis into mesenchymal cells or after neoplasia into invasive carcinoma cells. Of the syndecan family of transmembrane heparan sulfate proteoglycans, simple epithelia produce predominately syndecan-1, which is found at basolateral surfaces and within adhesive junctions. To elucidate the function of this syndecan-1, normal murine mammary gland epithelia were made deficient in syndecan-1 by transfection with an expression vector containing the syndecan-1 cDNA in the antisense configuration. Several independently derived clones of stable transfectants contained the antisense cDNA in their genome and expressed the antisense transcript. These grew either as epithelial islands of closely adherent polygonal cells, identical to both the parental cells and the vector-only control transfectants, or as individual elongated fusiform cells that invaded and migrated within collagen gels, like mesenchymal cells, but were anchorage-independent for growth. The clones that retained epithelial characteristics were moderately deficient in cell surface syndecan-1 (greater than 48% of control levels) but did not differ from control cells in expression of β1-integrins and E-cadherin, or in F-actin organization. However, the clones of fusiform cells were severely deficient in cell surface syndecan-1 (less than 12% of control levels) and showed rearranged β1-integrins, markedly reduced E-cadherin expression, and disorganized F-actin filaments, but retained mammary epithelial markers. Therefore, depleting epithelia of cell surface syndecan-1 alters cell morphology and organization, the arrangement and expression of adhesion molecules, and anchorage-dependent growth controls. Thus, cell surface syndecan-1 is required to maintain the normal phenotype of simple epithelia.

INTRODUCTION

The shape, adhesion, motility, and organization of metazoan cells are differentiated characteristics that determine cell behavior during morphogenesis and after neoplastic transformation. A large variety of molecules is involved in establishing and maintaining these characteristics. The initial morphology of differentiated cells in vertebrate embryos is epithelial, but the cells can transform during development into a mesenchymal phenotype in a highly regulated, spatiotemporal pattern (Hay, 1991). Such transformations are also part of wound repair, organ remodeling, and tumorigenesis and metastasis. The molecules involved in these epithelial-mesenchymal transformations are becoming increasingly understood.

Simple epithelia are sheets of cuboidal or columnar cells that show apical-basal polarity and lateral inter-

* Current address: Megabios Corporation, 863A Mitten Road, Burlingame, CA 94010.
† Corresponding author: Joint Program in Neonatology, Harvard Medical School, 300 Longwood Avenue, Boston, MA 02115.

cellular junctions, and lie sessile on a basement membrane. These characteristics are lost during their transformation into mesenchymal cells which, in typical fibroblastic cells, are elongated fusiform cells that migrate as single cells through the extracellular matrix (Hay, 1991). These cells have a leading edge, but do not form polarized membrane domains or adhesion junctions as in epithelia.

Some epithelial cells can be transformed into mesenchyme-like cells by modulating the cellular microenvironment. For example, when lens epithelia or thyroid follicles are embedded in a type I collagen gel, or MDCK cells precultured on basement membrane matrix are cultured on type I collagen gels, these epithelia transform into cells with a mesenchymal phenotype (Greenburg and Hay, 1986, 1988; Zuk *et al.*, 1989). Antibodies against E-cadherin or β1-integrins can disrupt epithelial monolayers causing the cells to become mesenchyme-like (Yoshida-Noro *et al.*, 1984; Behrens *et al.*, 1989; Hirai *et al.*, 1989; Larjava *et al.*, 1990; Symington *et al.*, 1993). For example, when treated with anti E-cadherin antibodies, MDCK cells that normally form typical epithelial sheets invade collagen gels or chick hearts, suggesting that they have acquired a mesenchymal phenotype (Behrens *et al.*, 1989). Growth factors can also regulate this transformation. For example, hepatocyte growth factor/scatter factor can mediate this transformation in several epithelial cell lines (Gherardi *et al.*, 1989; Weidner *et al.*, 1990). Exogenous acidic fibroblast growth factor induces an epithelial-mesenchymal transformation in a rat bladder carcinoma cell line (Vallés *et al.*, 1990). Overexpression of basic fibroblast growth factor causes rat pancreatic acinar epithelial cells to assume a fibroblastic shape (Estival *et al.*, 1993). Although the function of wnt-1 protein is unknown, this secreted protein can transform mammary epithelial cells into the mesenchymal phenotype (Jue *et al.*, 1992).

Thus, a variety of cell-cell, cell-matrix, and/or cell-growth factor interactions can induce epithelial-mesenchymal transformations. The cell surface molecules involved in these interactions differ widely, but the similarity of the response raises the possibility that a common post-receptor mechanism or a common coreceptor for growth factor, extracellular matrix, and cell adhesion molecules might be involved. Because of the evidence that cell surface proteoglycans function as coreceptors for each of these classes of molecules (Bernfield *et al.*, 1992), we have examined the possibility that epithelial-mesenchymal transformations involve a change in expression of these proteoglycans.

The major cell surface proteoglycan on epithelial cells is syndecan-1, a member of the syndecan family of transmembrane heparan sulfate proteoglycans (Bernfield *et al.*, 1992; Kim *et al.*, 1994). Syndecan-1 is a 31-kDa protein containing a 34-amino acid cytoplasmic domain, a transmembrane domain, and an extracellular domain bearing chondroitin sulfate chains near the plasma membrane and heparan sulfate chains near the N-terminus (Saunders *et al.*, 1989; Kokenyesi and Bernfield, 1994). Via its heparan sulfate chains, syndecan-1 binds cells to soluble and insoluble heparin-binding molecules such as interstitial collagens (Koda and Bernfield, 1984; Koda *et al.*, 1985), fibronectin (Saunders and Bernfield, 1988), thrombospondin (Sun *et al.*, 1989), tenascin (Salmivirta *et al.*, 1991), and basic fibroblast growth factor (Kiefer *et al.*, 1990; Bernfield and Hooper, 1991). The cytoplasmic domain of syndecan-1 associates with F-actin directly or indirectly when the extracellular domain is cross-linked by ligands (Rapraeger *et al.*, 1986), suggesting syndecan-1 may be involved in extracellular-intracellular signaling. Syndecan-1 localizes at the basolateral surfaces of epithelial cells (Rapraeger *et al.*, 1986; Hayashi *et al.*, 1987). This localization mimics that of E-cadherin (Takeichi, 1988), α2β1-, and α3β1-integrins (Larjava *et al.*, 1990; Symington *et al.*, 1993). The localization and embryonic distribution of syndecan-1 has previously suggested that it plays a pivotal role in maintaining epithelial morphology (Bernfield *et al.*, 1985).

We hypothesized that if syndecan-1 is involved in maintaining epithelial morphology and behavior, that its loss from epithelial cell surfaces would result in an epithelial-mesenchymal transformation. To test this hypothesis, we stably transfected a cell line that shows typical epithelial characteristics, normal murine mammary epithelial (NMuMG)[1] cells, with an antisense syndecan-1 RNA expression vector, and produced several clones of syndecan-1-deficient NMuMG cells. Here we report that syndecan-deficient NMuMG cells lose their epithelial phenotype and acquire mesenchymal morphology and behavior, as well as loss of anchorage-dependent growth. The results indicate that syndecan-1 is required to maintain the epithelial phenotype.

MATERIALS AND METHODS

Vector Construction

The *Sac*I-*Hin*dIII fragment (nucleotides 214-1379) of the murine syndecan-1 cDNA (Saunders *et al.*, 1989) in pGEM3Z (Promega, Madison, WI) was excised with *Eco*RI and *Hin*dIII, and ligated into Bluescript SK (Stratagene, La Jolla, CA). Subcloning into the multicloning site of Bluescript allowed excision of the insert as a *Hin*dIII-*Bam*HI fragment, which was then subcloned directionally, in an inverse 5′ to 3′ orientation with respect to the β-actin promoter, into the unique *Bam*HI-*Hin*dIII sites of the expression vector LK444 (Gunning *et al.*, 1987) to produce pMB9. The resultant vector contains 26-bp 5′-untranslated, 936-bp coding, and 204-bp 3′-untranslated sequences of the syndecan-1 cDNA. Plasmids were grown in TG-1 in the presence of 100 μg/ml of ampicillin and purified twice by isopycnic centrifugation in CsCl (Sambrook *et al.*, 1989).

[1] Abbreviations used: NMuMG, normal murine mammary gland; MMFG, mouse milk fat globule.

Cell Culture and Transfection

NMuMG cells (Owens *et al.*, 1974) were obtained from H.S. Smith (University of California, Berkeley, CA), and cultured in Dulbecco's modified Eagle's medium (DME) and fetal calf serum (FCS) as described elsewhere (David *et al.*, 1981). The cells were cloned twice in our laboratory, selecting for epithelial morphology, and clone 35 was used at passage 13–23 throughout the experiments described below. Twenty micrograms of pMB9 or LK444 was transfected into 70% confluent NMuMG cells by the calcium phosphate-mediated transfection/glycerol shock technique (Sambrook *et al.*, 1989). Subsequently, the cells were split and plated into five 100-mm dishes, and cultured after 48 h in the presence of 800 μg/ml G418 (Geneticin; Life Technologies, Gaithersburg, MD). During the following 3 wk, colonies of stable transfectants appeared on these secondary plates, and these were cloned with cloning rings.

Collagen Gel Invasion Assay

Type I collagen gels (0.25% wt/vol) in 24-well plates were formed by neutralizing rat tail tendon collagen (Collaborative Research, Bedford, MA) with $NaHCO_3$ in the presence of DME and FCS. Cell suspensions obtained by trypsinization were plated into wells (10^4 cells/well), cultured for 5 days at 37°C in 5% (vol/vol) CO_2, and photographed with a phase contrast-equipped Nikon Diaphot inverted microscope (Nikon, Tokyo, Japan). In some experiments, cell aggregates prepared by mechanical dispersal of confluent cell layers were embedded within collagen gels and cultured as described above.

Agarose Gel Colony Formation Assay

An agarose solution (0.5% wt/vol) made with SeaPlaque low melt agarose (FMC Bioproducts, Rockland, ME) in DME and FCS at 37°C was poured into 60-mm tissue culture dishes (6 ml per dish) and allowed to gel. Trypsinized cells suspended in 0.34% (wt/vol) agarose in DME and FCS were overlayed on the previously formed gels (1.5 ml per dish). The gel was allowed to form at room temperature, and the dishes were incubated at 37°C in 5% (vol/vol) CO_2 for 20 days. Phase contrast micrographs were taken for evaluation.

Genomic Southern Analysis

Genomic DNA was prepared from NMuMG cells and the transfectants by the proteinase K digestion/phenol-chloroform extraction method (Sambrook *et al.*, 1989). Approximately 10 μg genomic DNA was digested with *Eco*RI or *Hin*dIII at 37°C overnight, and subjected to 1% (wt/vol) SeaKem agarose (FMC Bioproducts, Rockland, ME) gel electrophoresis with 50 mM Tris-boric acid, pH 8.0, 1 mM EDTA. Fractionated DNA was transferred to Genescreen (DuPont NEN, Boston, MA), and hybridized with a [α-^{32}P]dCTP-labeled *Eco*RI-*Hin*dIII fragment of syndecan-1 cDNA, 4–19B containing the full coding region of syndecan-1 as described previously (Saunders *et al.*, 1989; Oettinger *et al.*, 1991). The membrane was subjected to autoradiography with Kodak XAR5 film (Eastman Kodak) at −70°C.

Northern Blot Analysis

Total RNA was prepared by the guanidine thiocyanate/CsCl ultracentrifugation method (Sambrook *et al.*, 1989). Ten micrograms of total RNA was fractionated with 1.2% (wt/vol) SeaKem agarose gel, and transferred to GeneScreen as described previously (Saunders *et al.*, 1989). The blots were hybridized with [α-^{32}P]CTP-labeled syndecan-1 sense or antisense RNA (prepared with SP6- or T7 RNA polymerase, respectively, on the *Eco*RI-*Hin*dIII fragment of 4–19B subcloned in pGEM3Z), with [α-^{32}P]dCTP-labeled cDNA for E-cadherin (a gift from Masatoshi Takeichi, Kyoto University, Japan), or mouse β-actin cDNA probe. The blot hybridized with syndecan-1 antisense RNA was treated with RNase A (5 μg/ml in 10 mM Tris-HCl, pH 8.0, 1 mM EDTA for 15 min at room temperature) to reduce the background caused by the nonspecific binding of the probe to the RNA samples. The membrane was subjected to autoradiography as above. In some experiments, the blot was stained with methylene blue to detect RNA (Sambrook *et al.*, 1989).

Antibodies and Immunofluorescent Microscopy

Antibodies used in this study were as follows: 281–2 is a rat mAb against the mouse syndecan-1 core protein (Jalkanen *et al.*, 1985); LE61 is a mAb against kangaroo rat cytokeratin 18 (Lane, 1982), and was a gift from E. Brigitte Lane (Imperial Cancer Research Fund, United Kingdom); rabbit anti-mouse milk fat globule (MMFG) antigen antibody was a gift from Roberto L. Ceriani (John Muir Cancer Research Institute, CA) (Ceriani and Peterson, 1978); rabbit anti-hamster vimentin antibody (Hynes and Destree, 1978) was a gift from Richard Hynes (Massachusetts Institute of Technology, Cambridge, MA); ECCD-2 is a rat mAb against mouse E-cadherin (Shirayoshi *et al.*, 1986), and was a gift from Masatoshi Takeichi (Kyoto University, Japan); and rabbit anti-human fibronectin receptor antibody was obtained from Telios Pharmaceuticals (San Diego, CA).

Cells were plated on cover slips (Bellco Glass, Vineland, NJ) and cultured for 2 days, at which time they were 50–90% confluent. In some experiments cells were cultured for 5 days after reaching confluence. For the immunostaining of syndecan-1, E-cadherin, and MMFG antigen, cells were fixed with freshly prepared 2% (wt/vol) paraformaldehyde in 1 mM $CaCl_2$, 0.5 mM $MgCl_2$, phosphate-buffered saline (mPBS) for 20 min, and permeabilized with 0.1% Triton X-100 in 0.15 M NaCl, 10 mM Tris-HCl, pH 7.4, 1 mM $CaCl_2$, 0.5 mM $MgCl_2$ (mTBS) for 5 min at room temperature. For the staining of cytokeratin 18, vimentin, and the fibronectin receptor, cells were fixed and permeabilized with ice-cold methanol for 10 min, and rehydrated with mTBS. Cells were blocked with 5% goat serum or swine serum in 0.1% bovine serum albumin in mTBS for 20 min, and incubated with first antibodies described above. After washing with mTBS, the cells were incubated with fluorescein isothiocyanate (FITC)- (Cappel, Durham, NC) or tetramethyl-rhodamine isothiocyanate (TRITC)-conjugated goat anti-rat IgG (Jackson Immunoresearch Laboratories, West Grove, PA) for syndecan-1 and E-cadherin, FITC-conjugated rabbit anti mouse-IgG (Accurate Chemicals and Scientific, Westbury, NY) for cytokeratin 18, and FITC-conjugated swine anti-rabbit IgG (Dako, Carpinteria, CA) for MMFG antigen, vimentin, and fibronectin receptor. FITC-conjugated phalloidin (Molecular Probes, Eugene, OR) was used to detect F-actin. Cells were mounted on glass slides with 0.1% (wt/vol) *p*-phenylenediamine, PBS, 90% (vol/vol) glycerol, and observed with an epifluorescent-equipped Axiophot microscope (Carl Zeiss, Thornwood, NY). The phase and immunofluorescent photomicrographs were taken with Tmax 400 film (Eastman Kodak, Rochester, NY) by automatic (for phase) or manual exposure (for fluorescence).

Quantitation of Cell Surface Syndecan-1

Syndecan-1 on the surface of cells grown in 60-mm dishes (50–90% confluent) was released with crystalline trypsin (Type VIII; Sigma, St. Louis, MO), and quantitated by radioimmunoassay with radioiodinated mAb 281–2 as described previously (Jalkanen *et al.*, 1987; Sanderson *et al.*, 1992). The cell pellet was dissolved in 0.2 M NaOH, and cellular protein was quantitated with BCA protein assay (Pierce, Rockford, IL) according to the manufacturer's instructions. Bovine serum albumin was used as a protein standard. The amount of syndecan-1 was normalized by the amount of the cellular protein.

Immunoprecipitation for Integrins

Cells (6×10^7 cells for ^{125}I, 6×10^6 cells for ^{35}S) were labeled chemically on their surfaces with 1.5 mCi of Na[^{125}I] (Dupont

NEN) by lactoperoxidase (Calbiochem, La Jolla, CA) (Morrison, 1974) or metabolically with 50 μCi/ml of [^{35}S]methionine (Tran^{35}S-label; ICN, Irvine, CA) for 16 h in methionine- and cysteine-free DME. After labeling, cells were extracted with 0.5% NP-40, 1 mM $CaCl_2$, 1 mM $MgCl_2$, TBS, 1 mM phenylmethylsulfonyl fluoride for 30 min at 0°C. After removing unincorporated radioactivity by Sephadex G-25 column chromatography (Pharmacia Biotech, Piscataway, NJ), the supernatants (5.0×10^5 cpm for ^{125}I, 4×10^7 cpm for ^{35}S) were subjected to immunoprecipitation with rabbit anti-chicken β1-, α3-, or α5-integrin antibodies (gifts from Richard Hynes) (Marcantonio and Hynes, 1988; Hynes *et al.*, 1989) and protein A agarose, and were fractionated by sodium dodecyl sulfate-polyacrylamide gel electrophoresis (SDS-PAGE) on 7.5% (wt/vol) gel with a discontinuous buffer system (Laemmli, 1970) under nonreducing conditions. The gels were dried and subjected to autoradiography (for ^{125}I) or fluorography with Enlightning (Dupont NEN). Densitometric analysis was performed in two dimension with a laser densitometer (Gelscan XL, Pharmacia Biotec).

Western Blot Analysis for E-Cadherin

Cells in 60-mm dishes (70–90% confluent) were lysed in 300 μl of 2% SDS, 1 mM $CaCl_2$, 50 mM Tris-HCl, pH 7.4, 5% (vol/vol) 2-mercaptoethanol, 0.025% bromophenol blue, and boiled for 10 min. The protein content of the cell lysates was determined by BCA assay after precipitating proteins in aliquots by 20% (wt/vol) trichloroacetic acid. Cell lysates (10 μg protein) were fractionated by SDS-PAGE as described above, and transferred to polyvinyliodine difluoride membranes (Immobilon-P; Millipore, Bedford, MA). The membranes were incubated with ECCD-2 (Shirayoshi *et al.*, 1986), alkaline phosphatase-conjugated goat anti-rat IgG (Caltag, South San Francisco, CA), and signals were detected by incubating the membrane with a mixture of nitroblue tetrazolium and 5-bromo-4-chloro-3-indolyl phosphate (Bio-Rad, Richmond, CA).

Statistical and Sequence Analyses

The means and standard deviations of the data were calculated with Microsoft Excel (Microsoft, Seattle, WA). The statistical significance (p value) of the data was calculated using a nonparametric Mann-Whitney test with Instat biostatistic program (GraphPad Software, San Diego, CA) on a Macintosh computer. Assessments of sequence homologies were based on rat sequences for syndecan-1 (syndecan; M81785), syndecan-2 (fibroglycan; M81687), and syndecan-4 (ryudocan; M81786) and performed with the GAP program in GCG sequence analysis software (Madison, WI).

RESULTS

NMuMG cells, initially obtained by selective trypsinization of normal mouse mammary epithelium (Owens *et al.*, 1974), were cloned by selecting for archetypical epithelial morphology, and then maintained at low culture densities and used at low passages (passage 13–23). When grown on tissue culture plastic, these NMuMG cells show characteristic epithelial morphology and growth pattern; at confluence, these cells form a continuous monolayer of polygonal cells, often forming domes that are characteristic of polarized epithelia in culture (David *et al.*, 1981). At subconfluence, they form islands of closely associated polygonal cells, and the cells at the edge of the islands spread smoothly contoured lamellipodia onto the surface of the plastic culture substratum. These NMuMG cells express the MMFG antigen, a differentiation marker for mammary epithelial cells, indicating that they maintain mammary epithelial differentiation (Ceriani and Peterson, 1978).

Syndecan-1 Antisense Transfectants Exhibit Two Distinct Morphologies

In an attempt to generate syndecan-deficient cells, a syndecan-1 antisense mRNA expression vector (pMB9) was constructed from the mammalian expression vector LK444 (Gunning *et al.*, 1987) by inserting the full coding region of syndecan-1 cDNA in the antisense configuration. LK444 and pMB9 were transfected into NMuMG cells, and cells resistant to G418 were cloned. Nine clones of LK444 transfectants were isolated and maintained (termed vector-only transfectants). Each isolate showed a morphology and growth pattern identical to those of the parental NMuMG cells whether in subconfluent or confluent culture (Figure 1, a and b).

The G418 resistant cells transfected with the pMB9 antisense construct showed two morphologically distinct sets of colonies. One set yielded typical epithelial clones that were indistinguishable from both the parental NMuMG cells and the vector-only transfectants in morphology and growth pattern, forming islands of closely associated polygonal cells when subconfluent (Figure 1c) and a continuous monolayer of polygonal cells when confluent (Figure 1d). These cells were termed epithelial antisense transfectants. The other set yielded clones of cells showing an elongated morphology and were termed fusiform antisense transfectants. These grew as individual cells in subconfluent culture with extensive filopodia that often under- or over-lapped adjacent cells (Figure 1, e and f). In confluent culture, these cells formed a continuous monolayer of morphologically heterogeneous cells that were often seen to over- or underlap other cells (Figure 1f, arrowheads).

From two independent transfections with pMB9, 25 G418-resistant clones were chosen and cloned. Of these, 18 clones showed epithelial morphology, eight clones of which were further characterized (E1.7, E1.8, E1.11, E1.12, E1.15, E1.18, E2.1, and E2.2; "E" indicates epithelial morphology, the first digit denotes first or second transfection experiment, and the second digit denotes clone number). The remaining clones showed fusiform morphology and all seven were further characterized (M1.4, M1.6, M1.9, M1.16, M2.6, M2.8, and M2.9; "M" indicates mesenchymal morphology). A single clone was selected from the vector-only transfectants (tLK1.12), and was used as a transfection control.

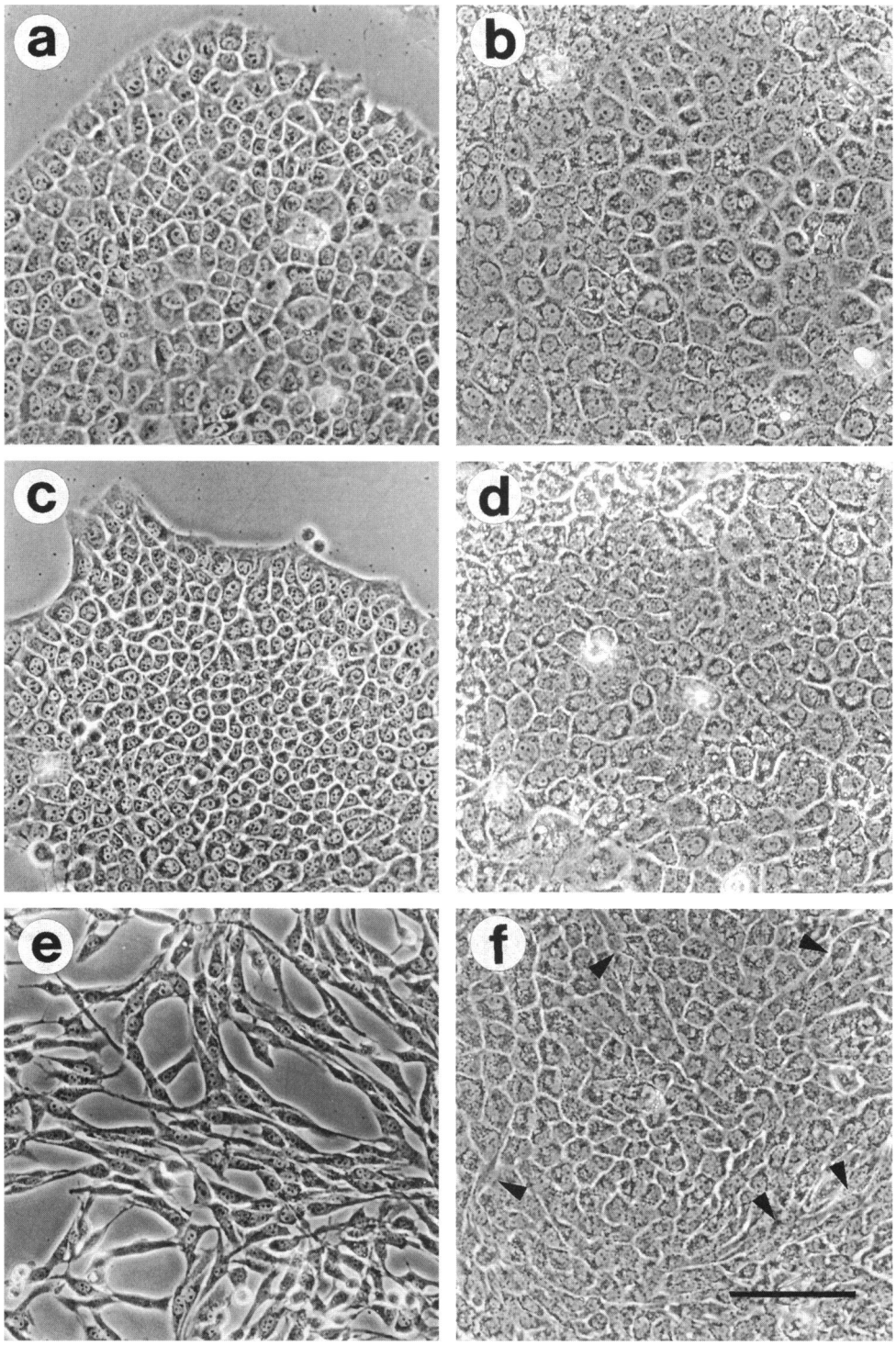

Figure 1. Syndecan-1 antisense cDNA transfectants show two distinct morphologies. The morphology on tissue culture plastic of the vector-only (tLK1.12; a and b), epithelial antisense (E1.8; c and d), and fusiform antisense (M1.4; e and f) transfectants was examined at subconfluence (a, c, and e) and 5 days postconfluence (b, d, and f). In panel f the cell processes that over- or underlap with other cells are marked with arrowheads. The other epithelial (E1.7, E1.11, E1.12, E1.15, E1.18, E2.1, and E2.2) and fusiform (M1.6, M1.9, M1.16, M2.6, M2.8, and M2.9) antisense transfectants showed morphologies indistinguishable from E1.7 and M1.4, respectively (not shown). Bar, 100 μm.

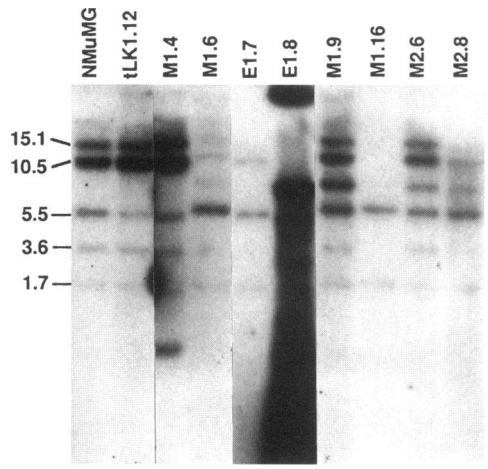

Figure 2. Cloned antisense transfectants are independent isolates. Southern analysis of DNA isolated from parental NMuMG cells, vector-only (tLK1.12), and antisense (M1.4, M1.6, E1.7, E1.8, M1.9, M1.16, M2.6, and M2.8) transfectants was performed using the *Eco*RI-*Hin*dIII fragment of mouse syndecan-1 cDNA, 4–19B, as a probe. The DNA was digested with *Eco*RI. The molecular sizes (kb) of restriction fragments from the endogenous *Synd1* gene are indicated.

Transfectants Contain Integrated Antisense Syndecan-1 cDNA

To establish whether the clones isolated after antisense transfections contained the antisense cDNA integrated into their genomes and were independent isolates, DNA prepared from these cells was digested with *Eco*RI or *Hin*dIII, and subjected to Southern blot analysis using mouse syndecan-1 cDNA as a probe (Saunders *et al.*, 1989). A representative blot from *Eco*RI digestions is shown in Figure 2. An integrated syndecan-1 antisense cDNA could not be identified in E2.1 and E2.2, and the Southern blot of DNA from M2.9 was found to be identical to that of M2.6. The remaining clones showed distinct restriction fragment patterns, indicating that they both contained the antisense DNA and were independent isolates. Restriction fragments derived from the endogenous *synd1* gene (Oettinger *et al.*, 1991) were not detected in some clones, presumably because the amount of DNA used was insufficient to detect the gene when present at only diploid levels. For further characterization, clones E1.7, E1.8, and E1.11 were chosen as typical representatives of the epithelial antisense transfectants and the clones M1.4, M1.6, M1.9, and M1.16 as typical representatives of the fusiform antisense transfectants.

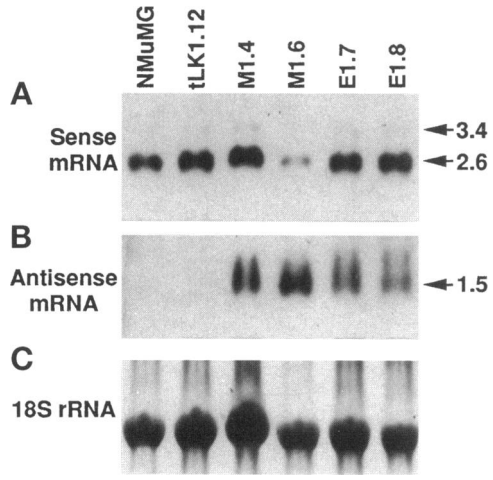

Figure 3. Antisense transfectants express antisense syndecan-1 mRNA. Total RNA prepared from parental NMuMG cells, vector-only (tLK1.12), and antisense transfectants (M1.4, M1.6, E1.7, and E1.8) was subjected to Northern blot analysis to detect syndecan-1 sense (A) and antisense mRNA (B) using syndecan-1 antisense and sense RNA probes, respectively. (C) The blot used to detect sense syndecan-1 mRNA was stained with methylene blue to show the abundance of 18 S RNA in the samples. Representative blots are shown. The molecular sizes (kb) of sense and antisense syndecan-1 mRNA are indicated.

Antisense Transfectants Express Antisense Transcripts

To assess whether the antisense transfectants express and accumulate both syndecan-1 sense and antisense mRNA, total RNA from the transfectant clones was subjected to Northern blot analysis. A mouse syndecan-1 antisense RNA probe detected similar levels of the native syndecan-1 sense transcripts in the parental NMuMG cells, the vector-only transfectant (tLK1.12), and in the M1.4, E1.7, and E1.8 antisense transfectants (Figure 3A); the M1.6 antisense transfectant contained a lower level. The 3.4-kb transcript was not as apparent as the 2.6-kb transcript, apparently because of its lower abundance (Saunders *et al.*, 1989). A mouse syndecan-1 sense RNA probe detected the syndecan-1 antisense transcript as a 1.5-kb transcript, smaller than the sense transcript because it is derived from the 1166-bp syndecan-1 antisense cDNA plus an SV40 polyadenylation cassette. This antisense transcript was detected solely in clones transfected with the pMB9 vector (M1.4, M1.6, E1.7, and E1.8, shown in Figure 3B as well as the fusiform antisense transfectants M1.9, M1.16, M2.6, and M2.8 [not shown]). Thus, these antisense transfectants express and accumulate syndecan-1 antisense mRNA, but there was no obvious relationship between the apparent levels of these transcripts and that of the native sense transcript, or a clone exhibited epithelial or fusiform morphology (cf. Figure 1).

Fusiform Antisense Transfectants Express a Reduced Level of Cell Surface Syndecan-1

To examine the relationship between cell surface syndecan-1 and cellular morphology and behavior, the

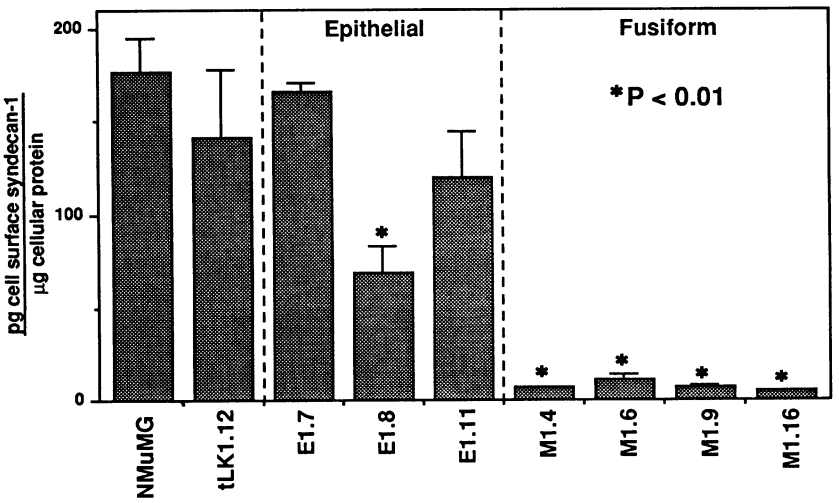

Figure 4. Fusiform antisense transfectants express a reduced amount of cell surface syndecan-1. Cell surface syndecan-1 was released by crystalline trypsin from the surfaces of parental NMuMG cells, vector-only (tLK1.1, 1.2, 1.3, 1.5, 1.6, 1.7, 1.9, 1.10, and 1.12), epithelial antisense (E1.7, E1.8, and E1.11), and fusiform antisense (M1.4, M1.6, M1.9, and M1.16) transfectants and quantitated by radioimmunodot assay. The amounts were normalized by the amount of cellular protein in each culture. Bars show mean ± SD for each clone (n = 3) except the vector-only transfectants represent the mean ± SD for the nine clones. Where indicated by asterisk, the difference from the vector-only transfectants is significant ($p < 0.01$).

amount of syndecan-1 on the surface of the antisense transfectants was quantitated (Figure 4). Cell surface syndecan-1 was quantitatively released from intact cells, assayed by 281–2 radioimmunoassay, and normalized for the amount of protein in the cells. The levels on the parental NMuMG cells and the vector-only transfectants (including tLK1.1, tLK1.2, tLK1.3, tLK1.5, tLK1.6, tLK1.7, tLK1.9, tLK1.10, and tLK1.12) were indistinguishable, indicating that the transfection and cloning did not affect the amount of cell surface syndecan-1. The epithelial transfectants (E1.7, E1.8, and E1.11) showed variable levels of cell surface syndecan-1 but none expressed less than 48% of the level on the vector-only transfectant controls. In contrast, the fusiform transfectants (M1.4, M1.6, M1.9, and M1.16) expressed uniformly low amounts of cell surface syndecan-1, each less than 12% of the control level ($p < 0.01$). These data indicate that the fusiform transfectants are deficient in cell surface syndecan-1 and that markedly reduced levels of cell surface syndecan-1 are associated with alterations in cell morphology and behavior.

Table 1. Confluent density and doubling time of transfectants.

Transfectants	Morphology	Cell number at confluence (mean ± SD × 10^6)	Doubling time (h)
tLK1.12	Epithelial	1.18±0.27	10.3
E1.8	Epithelial	1.14±0.15	11.4
M1.4	Fusiform	1.57±0.11*	13.0
M1.6	Fusiform	3.43±0.59**	12.3

Cells were plated in 24-well culture plates at day 0, and harvested by trypsinization at 24-h intervals up to 8 days. Cell number was determined using a hemocytometer (n=4).

*p <0.002.

**p <0.0001.

Growth Characteristics of Epithelial and Fusiform Antisense Transfectants

The growth rate and confluent density of the vector-only control and antisense transfectants were compared. Although each cell type (clones tLK1.12, M1.4, M1.6, and E1.8) grew with a similar doubling time (11.7 ± 1.2 h), their density at confluence differed (Table 1). At confluence the density of the vector-only transfectant tLK1.12 (1.2×10^6 cells/dish) was indistinguishable from that of the epithelial transfectant E1.8 (1.1×10^6 cells/dish), whereas fusiform transfectants M1.4 (1.6×10^6 cells/dish) and M1.6 (3.4×10^6 cells/dish) grew to a significantly higher cell density ($p < 0.002$). This higher density at confluence of the fusiform transfectants may be due to their under- and overlapping, as described above (cf. Figure 1).

Syndecan-1-deficient Antisense Transfectants Show Mesenchymal Cell Behavior and Anchorage-independent Growth

To evaluate their behavior when grown in association with an extracellular matrix or a nonadhesive substratum, the transfectants were cultured on top of type I collagen gels and within agarose gels, and as pre-formed aggregates within type I collagen gels. When vector-only transfectants were plated on top of the collagen gel, they grew on the gel surface as closely packed islands of polygonal cells (Figure 5a). Plated identically, the epithelial antisense transfectants were indistinguishable in morphology and behavior from the vector-only transfectants (Figure 5b). In contrast, when fusiform transfectants were plated on collagen gels, they became more spindle-shaped, showed extensive under- or over-lapping of filopodia, and migrated on the collagen gel as individual cells (Figure 5c). Furthermore, a large proportion of the cells emigrated from the gel surface

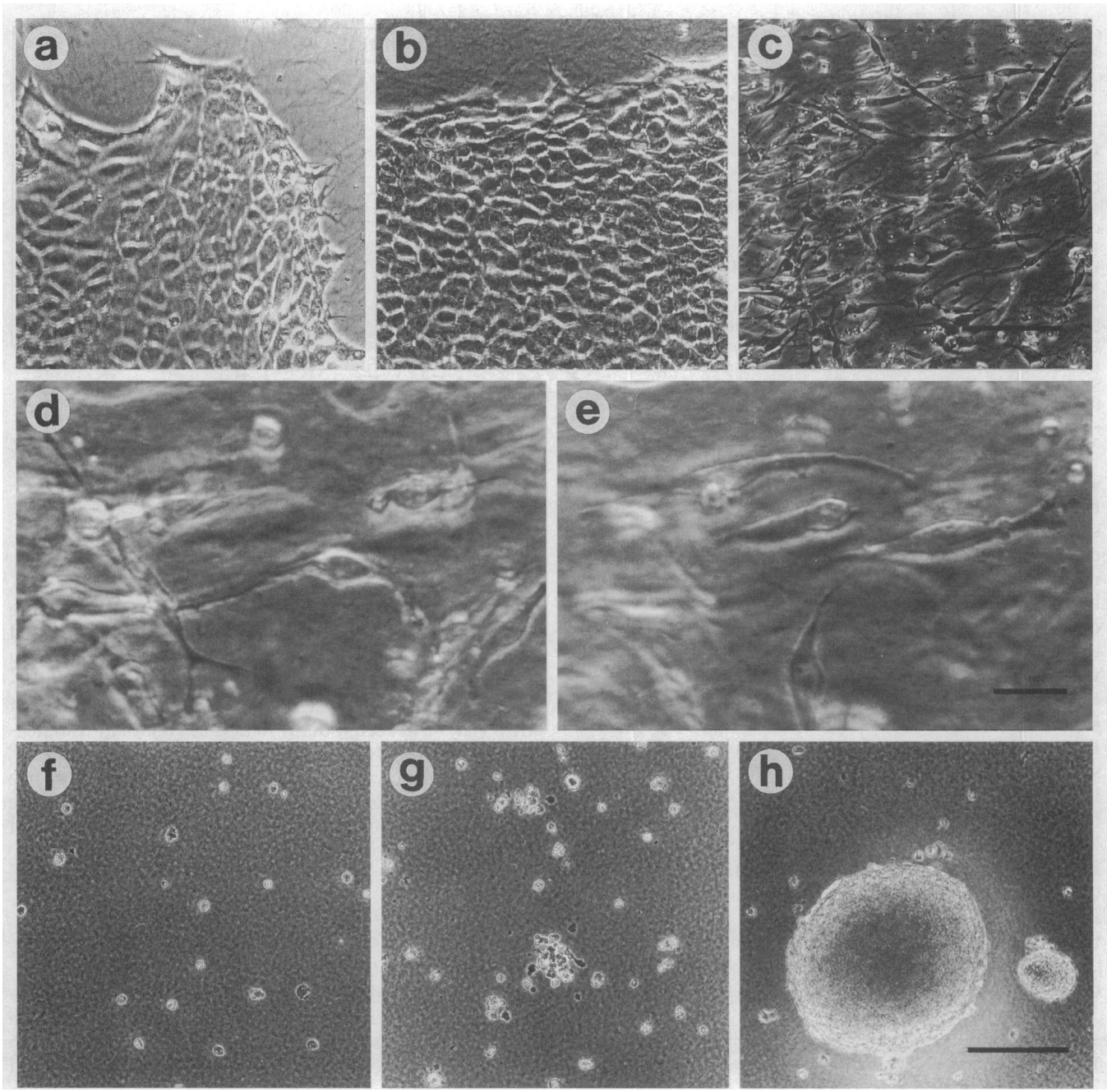

Figure 5. Fusiform antisense transfectants acquire mesenchymal cell behavior and anchorage-independent growth. Vector-only tLK1.12 (a and f), epithelial antisense transfectant E1.8 (b and g), and fusiform antisense transfectant M1.6 (c–e and h) were cultured on the surface of type I collagen gels (a–e), or within agarose gels (f–h). A higher magnification view of M1.6 migrating on the surface of collagen gels (d), and in the same field, 80 μm below the surface (e). E1.7 and M1.4 showed similar behavior to E1.8 and M1.6, respectively (not shown). Bars in a–c, d and e, and f-h correspond to 100 μm, 25 μm, and 200 μm, respectively.

and invaded the gel. Fusiform antisense transfectants were seen at least 80 μm below the surface of the collagen gel (Figure 5, d and e). When aggregates of vector-only and epithelial transfectants were cultured within collagen gels, they extended multicellular duct-like structures into the surrounding gel, as previously described (not shown; Hall *et al.*, 1982). However, within collagen gels, the aggregates of fusiform transfectants yielded cells that migrated individually into the gel (not shown). These results indicate that the epithelial transfectants behave on and within the collagen gel as de-

scribed for epithelial cells, whereas the fusiform transfectants exhibit the migratory behavior expected for mesenchymal cells.

The transfectants showed a major difference in viability when cultured within agarose gels. When the cells were embedded within the gels and cultured, both vector-only transfectants and epithelial antisense transfectants failed to proliferate and died (Figure 5, f and g), indicating that they retained anchorage-dependent growth characteristics. However, when cultured within gels, the fusiform transfectants remained viable, proliferated, and formed spherical colonies (Figure 5h), indicating that they acquired anchorage-independent growth characteristics.

Fusiform Antisense Transfectants Retain Mammary Epithelial Differentiation

To assess whether the morphological changes associated with syndecan-1 deficiency affected the capacity of the NMuMG cells to retain mammary epithelial characteristics, we evaluated their expression of the MMFG antigen and cytokeratin 18 as mammary and epithelial differentiation markers, and of vimentin, an intermediate filament that is characteristic of mesenchymal cells. The MMFG antigen, cytokeratin 18, and vimentin were observed in their usual intracellular localizations as previously described (Ceriani and Peterson, 1978; Hynes and Destree, 1978; Lane, 1982), and were distributed similarly in each transfectant (not shown). Indeed vimentin was expressed even in the parental cells, as is sometimes seen in cultured cells that otherwise have epithelial characteristics (Zuk *et al.*, 1989). Thus, despite the morphological change from epithelial to fusiform morphology, the fusiform antisense transfectants retain mammary epithelial differentiation markers.

Fusiform Antisense Transfectants Show Rearranged F-Actin Bundles

Syndecan-1 and F-actin have been shown to co-localize in NMuMG cells (Rapraeger *et al.*, 1986). Thus, we searched for this co-localization in vector-only, epithelial antisense, and fusiform antisense transfectants by staining with mAb 281–2 and with FITC-conjugated phalloidin (Figure 6). In sub-confluent cultures, syndecan-1 and F-actin colocalized at lateral cell surfaces at sites of cell-cell contact in the vector-only transfectants (Figure 6, a and b), in patterns identical to those described previously (Rapraeger *et al.*, 1986). Epithelial antisense transfectants showed the identical patterns (Figure 6, c and d). In fusiform antisense transfectants, the trace amount of cell surface syndecan-1 was detected in a punctate manner (Figure 6e), and only cortical F-actin staining was seen; this F-actin staining did not co-localize with the syndecan-1 (Figure 6, e and f). Interestingly, despite the fusiform morphology and mesenchymal cellular behavior, F-actin in these cells did not organize into stress fibers or insert into focal contacts. In post-confluent cultures, the distribution of syndecan-1 and F-actin did not change in the vector-only and epithelial antisense transfectants. However, after confluence the fusiform antisense transfectants acquired bundles of F-actin at their lateral cell surfaces at sites of cell contact (not shown).

Fusiform Antisense Transfectants Rearrange, but Do Not Change the Expression Level of β_1-integrins

Because the fusiform antisense transfectants show reduced cell-cell and cell-matrix adhesion (cf. Figures 1 and 5), we asked whether the reduced expression of syndecan-1 affected the expression and organization of other cell-cell and/or cell-matrix adhesion molecules. We first examined the expression of β1-integrins by immunofluorescent staining of permeabilized cells with an anti-human fibronectin receptor antibody that reacts with the β1-integrin subunit. In vector-only and epithelial transfectants, β1-integrins localized at lateral cell surfaces at sites of cell-cell contact (Figure 7, a–d) where α2β1 and α3β1 integrins are known to accumulate. This pattern is very similar to that of syndecan-1 and F-actin (cf. Figure 6). In fusiform antisense transfectants, however, punctate staining was observed in perinuclear areas and β1-integrins were not seen at cell-cell contact sites (Figure 7, e and f).

To assess whether the change in β1-integrin staining was due to altered expression, parental NMuMG cells, vector-only, epithelial, and fusiform antisense transfectants were radioiodinated on their surfaces with lactoperoxidase or metabolically labeled with [^{35}S]methionine, and extracted with NP-40 containing buffer. Equal amounts of radioactive cell extract were subjected to immunoprecipitation with antibodies against chicken β1-, α3-, or α5-integrins, and analyzed by nonreducing SDS-PAGE (Figure 8). The anti-β1 integrin antibody immunoprecipitated typical integrin heterodimers from both ^{125}I- and ^{35}S-labeled extracts; β1 and apparently multiple α subunits were seen at apparent molecular sizes of 127 and 145–150 kDa, respectively. Densitometric analyses indicated that the parental NMuMG cells express more of the β1 subunit, both total and at the cell surface, than the transfectants (Table 2). The level of the β1-subunit varied among the transfectants, but there was no relationship between this level and cell morphology or behavior. The α3- and α5-integrin antibodies immunoprecipitated amounts of β1-integrins that were also unrelated to cell morphology or behavior, suggesting no detectable change in β1-integrin repertoire (not shown). Although transfection, selection, and cloning reduced the amount of β1-integrins, no quantitative differences

in β1-integrins were detected among the transfectants. Thus, the altered immunostaining of β1-integrins on the fusiform transfectants (Figure 8) appears to be due to a redistribution rather than a change in the amount of cell surface β1-integrins.

Fusiform Antisense Transfectants Show Reduced Expression of E-Cadherin and Its Transcript

To assess E-cadherin expression, ECCD-2, a monoclonal antibody against mouse E-cadherin, was used for immunofluorescent staining (Figure 9) on permeabilized cells. In vector-only and epithelial transfectants, E-cadherin localized at lateral surfaces at sites of cell-cell contact, very similar to that of syndecan-1, F-actin, and β1-integrins (Figure 9,a–d; cf. Figures 6 and 7). In contrast, meager staining was observed in fusiform antisense transfectants, suggesting little or no expression of E-cadherin (Figure 9, e and f). This result was confirmed by Western blot analyses for E-cadherin (Figure 10A). The parental NMuMG cells, vector-only, and epithelial antisense transfectants expressed nearly equal amounts of E-cadherin (molecular size 124 kDa), whereas fusiform antisense transfectants did not express detectable amounts.

To assess whether E-cadherin mRNA is also reduced in the fusiform antisense transfectants, the total RNA from NMuMG cells and transfectants was analyzed by Northern blotting with an E-cadherin cDNA probe (Figure 10B). Parental NMuMG cells, vector-only, and epithelial antisense transfectants expressed

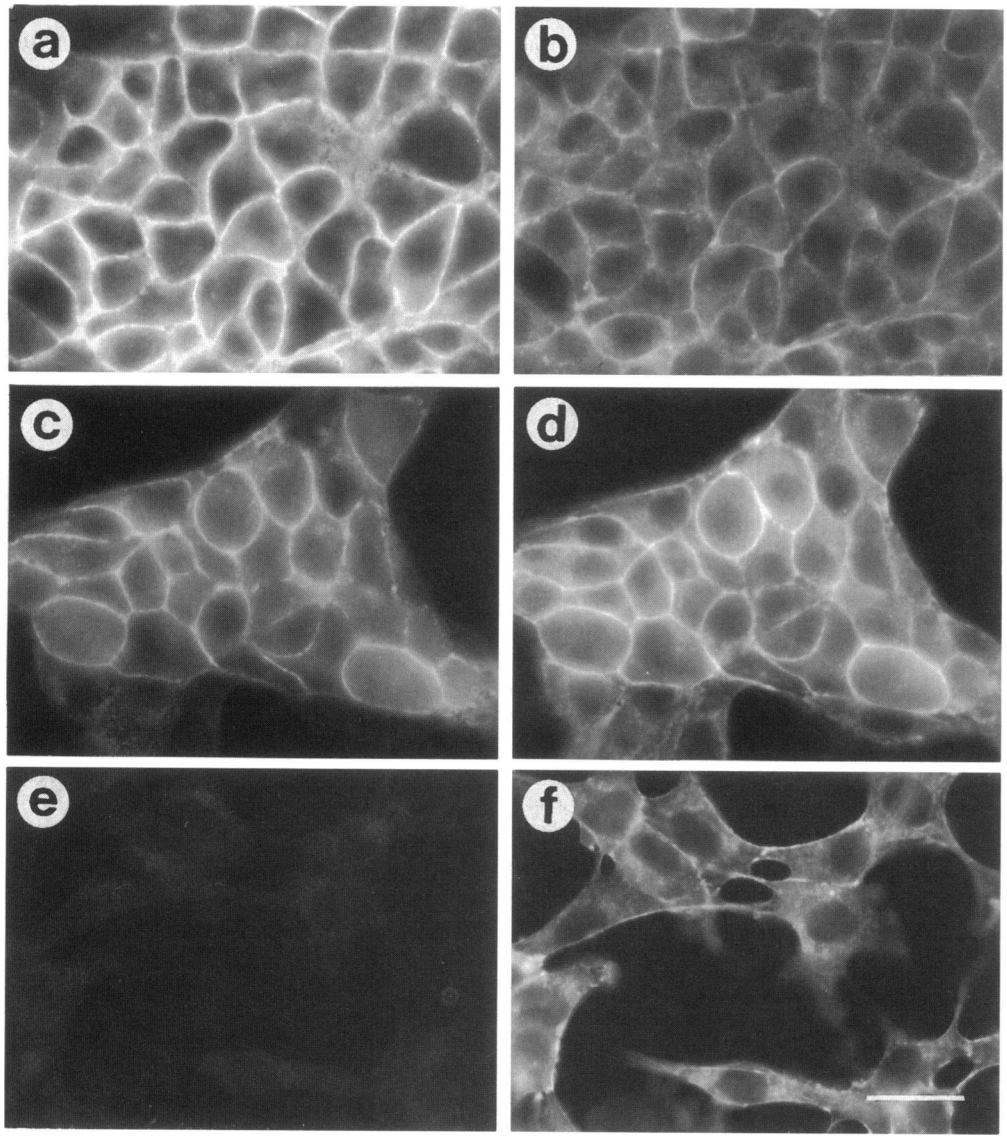

Figure 6. Fusiform antisense transfectants show reduced syndecan-1 and disorganized F-actin bundles. The vector-only transfectant tLK1.12 (a and b), epithelial antisense transfectant E1.7 (c and d), and fusiform antisense transfectant M1.6 (e and f) were permeabilized and double stained to detect syndecan-1 (a, c, and e) and fibrillar β-actin (b, d, and f). E1.8 and M1.4 showed similar staining patterns to E1.7 and M1.6, respectively (not shown). Bar, 25 μm.

nearly equal amounts of E-cadherin mRNA, however, little or no E-cadherin mRNA was detected in fusiform antisense transfectants. Thus, the fusiform antisense transfectants appear to contain markedly reduced levels of the E-cadherin transcript.

DISCUSSION

Syndecan-1, the major transmembrane heparan sulfate proteoglycan of epithelial cells, polarizes to the basolateral surface of epithelia both in vivo and in vitro. This paper describes syndecan-1–deficient epithelial cells generated by transfecting NMuMG mammary epithelial cells with an antisense syndecan-1 mRNA expression vector. Several stable transfectants expressing different amounts of syndecan-1 on their surfaces were obtained; each was shown to be an independent isolate, to contain the transfected syndecan-1 antisense cDNA in its genome, and to express an antisense transcript. Transfectants that were moderately deficient in syndecan-1 retained the epithelial morphology and culture behavior of the parental NMuMG cells. However, transfectants that were severely deficient in syndecan-1 lost the epithelial characteristics of their parental cells and acquired an elongate fusiform morphology, the ability to invade and migrate within collagen gels, and anchorage-independent growth. The fusiform antisense transfectants showed rearranged β1-integrins, markedly reduced E-cadherin expression, and altered disposition of the actin cytoskeleton. Despite differences from

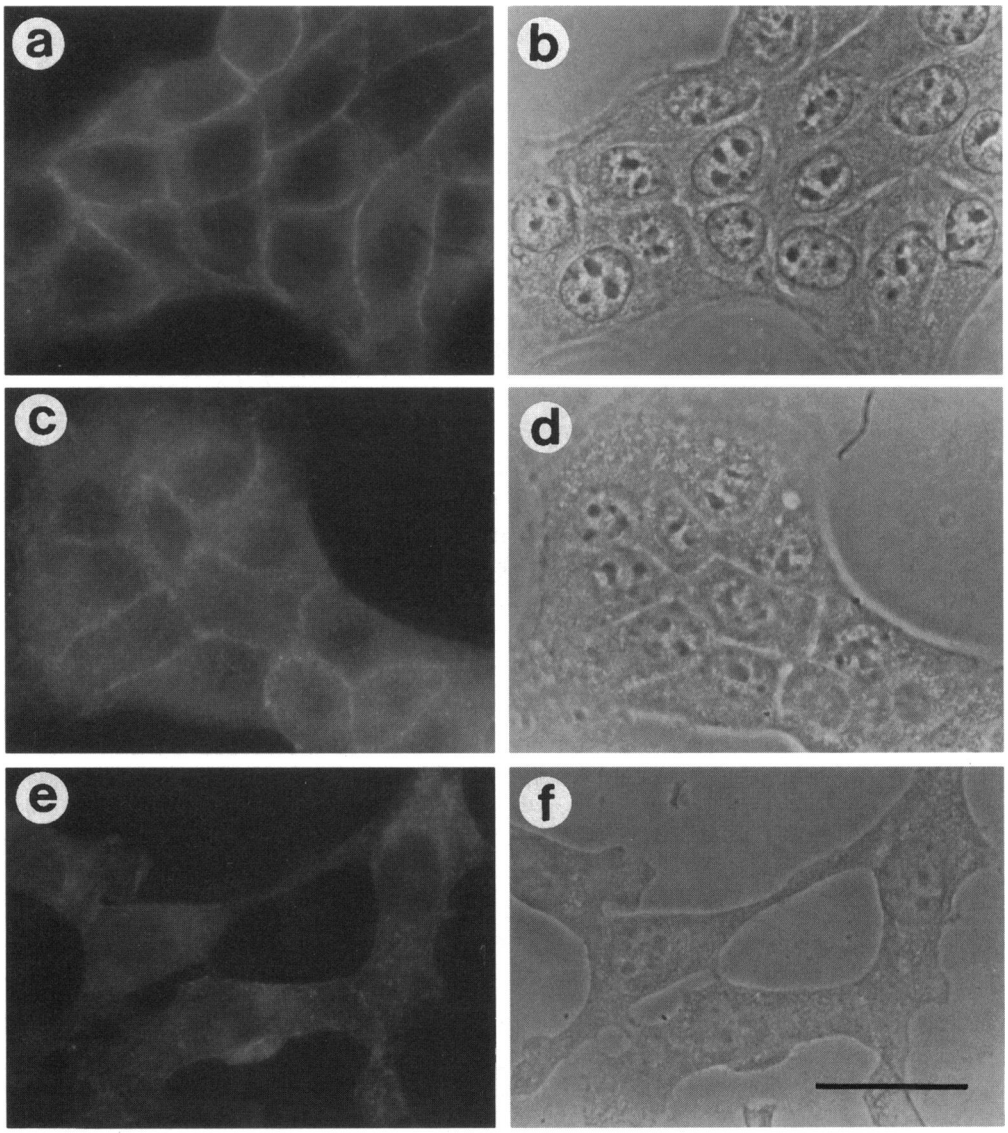

Figure 7. Fusiform antisense transfectants show a change in β1-integrin distribution. The vector-only transfectant tLK1.12 (a and b), epithelial antisense transfectant E1.7 (c and d), and fusiform antisense transfectant M1.6 (e and f) were permeabilized and immunostained to detect β1-integrins (a, c, and e), and observed by phase contrast microscopy (b, d, and f). E1.8 and M1.4 showed similar staining patterns to E1.7 and M1.6, respectively (not shown). Bar, 25 μm.

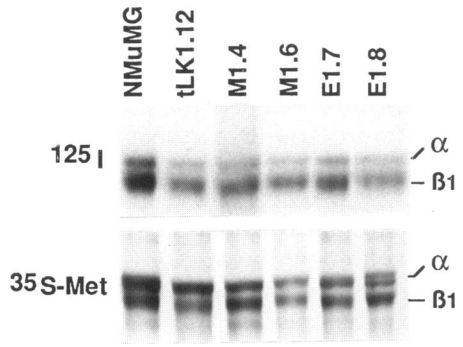

Figure 8. Fusiform antisense transfectants show no change in β1-integrin expression at the cell surface. Parental NMuMG cells, vector-only transfectant tLK1.12, fusiform antisense transfectants M1.4 and M1.6, and epithelial antisense transfectants E1.7 and E1.8 were radioiodinated on their surfaces with lactoperoxidase (^{125}I) or metabolically labeled with [^{35}S]methionine ([^{35}S]Met), and immunoprecipitated with antibodies against integrin β1-subunit. The immunoprecipitates were fractionated by nonreducing SDS-PAGE, and subjected to autoradiography (for ^{125}I) or fluorography (for ^{35}S).

their epithelial counterparts in morphology, cellular organization, adhesion, and cytoskeletal components, the fusiform antisense transfectants maintained differentiation markers for mammary epithelia. These results provide experimental evidence that confirms our previous proposal that syndecan-1 maintains epithelial morphology and organization (Bernfield, 1985).

Syndecan-1-deficient Cells Are Derived from Expression of the Syndecan-1 Antisense RNA

NMuMG cells were originally cultured from mammary explants and cloned for epithelial morphology and behavior (Owens *et al.*, 1974). Although they can be pleomorphic in culture, and clonal variants could exist that have lost both syndecan-1 and E-cadherin expression, no NMuMG cells have shown fusiform morphologies in our lab since being obtained in 1977 (David and Bernfield, 1979) and continuously maintained at low culture densities. Each transfectant clone studied here was resistant to a high concentration of G418 (800 μg/ml); each was demonstrated to be an independent isolate and to contain the antisense cDNA integrated into their genome (Figure 2). Both sham transfection and vector-only transfection followed by G418 selection of greater than 10^8 cells failed to yield a single fusiform colony (Kato and Bernfield, unpublished results). Moreover, we studied only those clones that were shown to express an antisense syndecan-1 transcript (Figure 3). Although several such clones were isolated, only those with low syndecan-1 expression showed reduced E-cadherin and were fusiform; others showed little change in E-cadherin and an epithelial phenotype. Thus, we conclude that the transfectants studied here are not clonal variants such as the fusiform-appearing cells (NM-f cells) directly cloned from NMuMG cells obtained from the ATCC (Vleminckx *et al.*, 1991).

The fusiform cells are all transfectants containing an altered genome, but integration of the antisense construct into a unique region of the genome cannot account for the syndecan-1 deficiency or for the change in phenotype of the cells. As demonstrated by restriction enzyme analyses, each of the antisense transfectants characterized here had integrated the antisense DNA into a different site in the genome (Figure 2). Thus, the syndecan-1 deficiency and the phenotypic effect are due to the antisense transcription product.

How the antisense transcript reduces the level of cell surface syndecan-1 is not wholly clear. Differences between transfectants in the level of antisense transcript can arise from variations in the number and site of the integrated antisense cDNA. Although the apparent amount of antisense transcript in these cells varied, as evaluated by Northern blots, these levels did not correlate with the apparent amount of syndecan-1 mRNA (Figure 3). This result is consistent with several reports in which transfection with antisense cDNA yields an antisense RNA that has little apparent effect on mRNA abundance, but substantially reduces the level of the translation product (Amini *et al.*, 1986; Wenz *et al.*, 1992; Godson *et al.*, 1993). Several mechanisms for this reduction are possible, including enhanced degradation or decreased transport into the cytoplasm of the sense-antisense duplex, or reduced core protein translation due to altered binding of the mRNA to the ribosome or another part of the translational machinery, or a combination of these. These mechanisms acting to different extent could account for the

Table 2. Relative abundance of integrin β1-subunit immunoprecipitated from cell surface-(^{125}I) or total- ([^{35}S]Met) labeled cells by anti-β1-integrin antibody.

		Relative Abundance of β1-subunit (%)	
Cells	Morphology	Cell surface (^{125}I)	Total ([^{35}S]Met)
NMuMG	Epithelial	100	100
tLK 1.12	Epithelial	48	69
M1.4	Fusiform	62	86
M1.6	Fusiform	38	35
E1.7	Epithelial	59	57
E1.8	Epithelial	38	58

The autoradiogram and fluorogram (see Figure 8) were subjected to densitometric analysis, and the intensity of the β1-subunit signal was quantitated. The relative abundance was calculated by setting the intensity of β1-subunit in NMuMG cells as 100%.

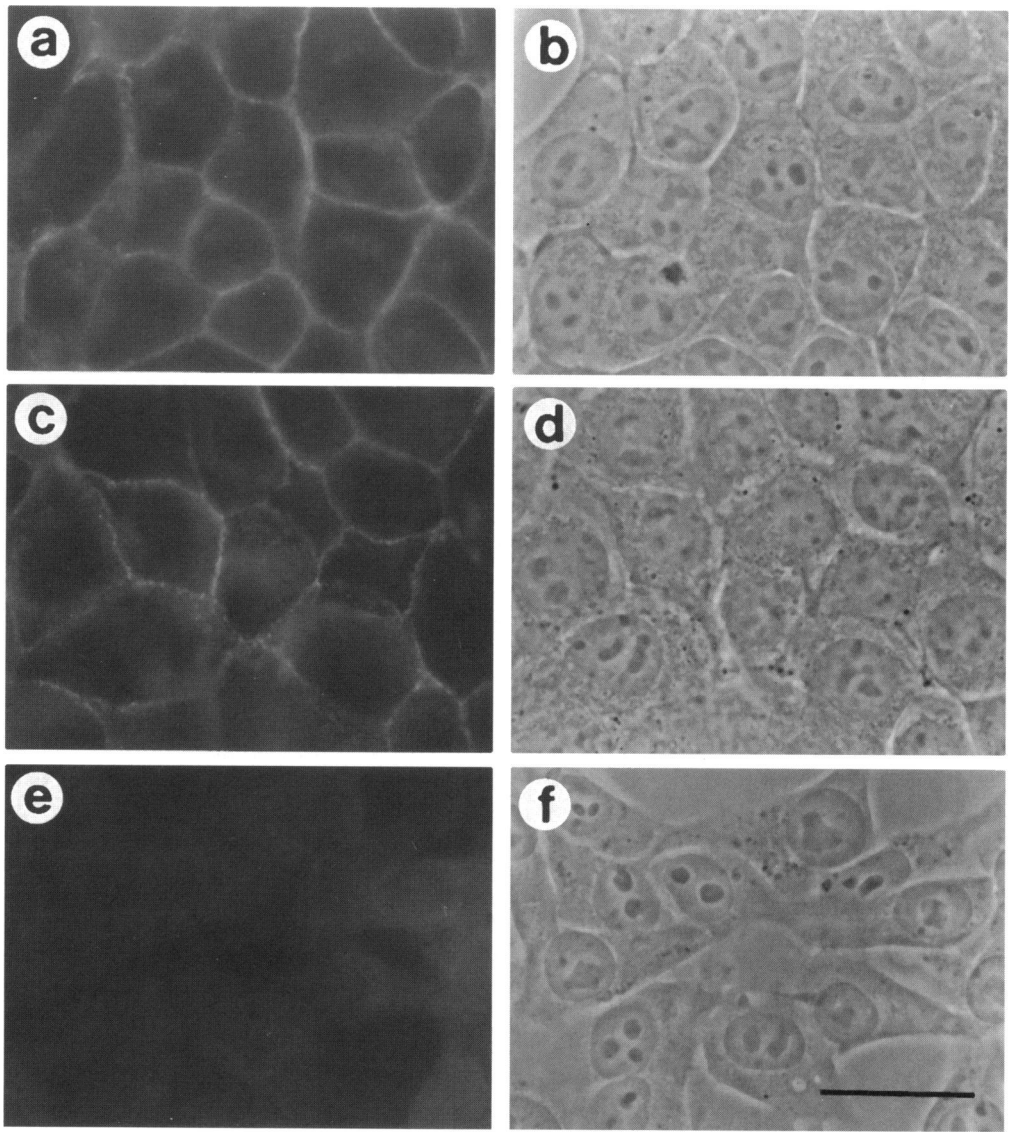

Figure 9. Localization of E-cadherin in syndecan-1 antisense transfectants. The vector-only transfectant tLK1.12 (a and b), epithelial antisense transfectant E1.7 (c and d), and fusiform antisense transfectant M1.6 (e and f) were permeabilized and immunostained to detect E-cadherin (a, c, and e), and observed by phase contrast microscopy (b, d, and f). E1.8 and M1.4 showed similar staining pattern to E1.7 and M1.6, respectively (not shown). Bar, 25 μm.

variation between the antisense transfectants in their level of cell surface syndecan-1.

NMuMG cells express multiple cell surface heparan sulfate proteoglycans, including glypican (Bernfield, unpublished results), syndecan-1, -2, and -4 (Lories *et al.*, 1992; Kim *et al.*, 1994). The antisense syndecan-1 transcript would not form duplexes with the transcripts coding for these proteoglycans and thus would not affect their level of expression. The nucleotide sequence of the glypican transcript is not homologous, and those for syndecan-2 and -4 are ca. 40% homologous to that of syndecan-1. However, these sequences have four (syndecan-2) and five (syndecan-4) significant gaps and the longest homologous stretch is 12 nucleotides. Indeed, Northern blot analyses using an antisense syndecan-1 RNA probe fail to show cross-hybridization with the syndecan-2 and -4 transcripts. Because the syndecan-1 transcript is most abundant in these cells, even if the other transcripts showed sufficient homology, the syndecan-1 sense-antisense duplex would predominate.

Abundance of Cell Surface Syndecan-1 Correlates with the Morphology, Organization, and Behavior of Epithelial Cells

The level of cell surface syndecan-1 was assessed specifically (as the assay depends on the reactivity of mAb 281–2) (Jalkanen *et al.*, 1985), accurately (as trypsin releases the syndecan-1 extracellular domain quantitatively) (Jalkanen *et al.*, 1987; Sander-

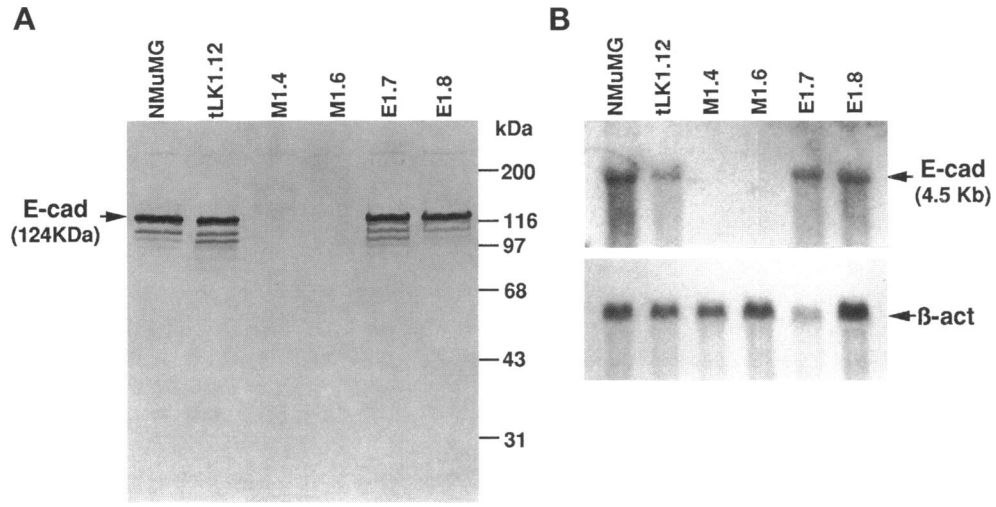

Figure 10. Fusiform antisense transfectants show reduced expression of E-cadherin and its transcript. (A) Parental NMuMG cells, vector-only transfectant tLK1.12, fusiform antisense transfectants M1.4 and M1.6, and epithelial antisense transfectants t1,7 and E1.8 were solubilized with SDS-PAGE sample buffer containing 1 mM $CaCl_2$, and subjected to Western blot analysis to detect E-cadherin with mAb ECCD-2 against E-cadherin. The bands marked by arrowheads are proteolytic products of E-cadherin as described previously (Shirayoshi *et al.*, 1986). The positions for molecular size markers (kDa) are indicated. Results obtained with E1.7 and 1.8 were also seen with E1.11, E1.12, E1.15, and E1.18, and results obtained with M1.4 and M1.6 were also seen with M1.9, M1.16, M2.6, and M2.8 (not shown). (B) Northern blot analysis to detect E-cadherin transcripts. Total RNA prepared from parental NMuMG cells, vector-only transfectant tLK1.12, fusiform antisense transfectants M1.4 and M1.6, and epithelial antisense transfectants t1,7 and E1.8 were subjected to Northern blot analysis to detect E-cadherin mRNA with an E-cadherin cDNA probe. The same blot was reprobed with a β-actin cDNA to show the abundance of β-actin mRNA in the samples.

son *et al.*, 1992), and reproducibly (as the same results were obtained over a 4-mo interval during which the cells were cultured in the presence of G418). The levels were normalized to cellular protein to minimize possible influences of differences in cell size or shape.

Transfectants showing more than 48% of the control level of cell surface syndecan-1 had the characteristics of their parental epithelial cells (Figure 4). In contrast, transfectants showing less than 12% of the control level of cell surface syndecan-1 retained certain mammary epithelial characteristics, viz. the MMFG antigen and cytokeratins, but had several features reminiscent of both mesenchymal and neoplastically transformed cells: individual spindle-shaped cells containing elongated filopodial extensions that under- or overlapped adjacent cells, and showing neither stress fibers nor focal adhesions (Figures 1 and 6). These cells grew at the same rate as their epithelial counterparts but to higher confluent densities, and most distinctly, were anchorage independent for growth and invaded into and migrated within collagen gels (Table 1 and Figure 5). After 5 to 7 days at confluence these fusiform antisense transfectants were less elongate and showed F-actin partly organized into circumferential bundles, especially evident at sites of cell-cell contact. But they showed no changes in their levels of either cell surface syndecan-1 or E-cadherin and still under- or overlapped adjacent cells, and invaded and migrated within collagen gels.

These data indicate that syndecan-1 is required to maintain epithelial morphology, organization, and behavior. Other recent studies are consistent with this conclusion. Androgen treatment of the S115 mouse mammary tumor cell line, which has an epithelial-like morphology, reduced the expression of syndecan-1 and promoted a more fusiform morphology, more rapid growth, and anchorage-independence (Leppä *et al.*, 1991). When a syndecan-1 cDNA under a glucocorticoid responsive promoter was introduced into these cells, hormone-induced expression of syndecan-1 prevented this change in phenotype (Leppä *et al.*, 1992). Expression of syndecan-1 in Schwann cells that normally do not express it correlates with a cytoskeletal reorganization and a more flattened and cuboidal morphology, both producing a morphology that is reminiscent of epithelial cells (Carey *et al.*, 1994). Further, in normal cells fibroblastic morphology and behavior correlate with low levels of cell surface syndecan-1; both cultured fibroblasts and epithelia express syndecan-1, but unlike epithelia, where it is abundant at the cell surface, it is predominantly intracellular in fibroblasts (Kato and Bernfield, unpublished observations).

Syndecan-1 Deficiency Accompanies Epithelial-Mesenchymal Transformations In Vivo

The morphologic transformation accompanying reduced syndecan-1 in cultured cells is similar to epithelial-mesenchymal transformations in vivo. For example, the keratinocytes at the lateral edges of repairing skin wounds in mice lose cell surface syndecan-1 and then change shape and migrate beyond the margin and into the wound (Elenius *et al.*, 1991). During murine development, syndecan-1 is initially

expressed at the 4-cell stage and remains expressed on the epithelial cell sheets that will become the embryo (Sutherland *et al.*, 1991). However it is lost at several sites where the cells become mesenchymal, as during the dispersion of the somite epithelium into sclerotome, dermatome, and myotome. During development of the secondary palate, the medial edge epithelia of the nasal and maxillary processes transform into mesenchymal cells (Fitchett and Hay, 1989). Immediately before this transformation and precisely at the sites where the epithelia will become mesenchymal cells, syndecan-1 expression is markedly reduced, and simultaneously E-cadherin expression decreases (McAlmon, 1992).

Taken together, loss of syndecan-1 expression appears to be associated with a change in morphological differentiation. Interestingly, once lost, the reexpression of syndecan-1 does not routinely restore epithelial morphology. Intense expression of cell surface syndecan-1 in several embryonic mesenchymal tissues does not cause them to become epithelial in morphology or organization (Thesleff *et al.*, 1988; Solursh *et al.*, 1990; Sutherland *et al.*, 1991; Trautman *et al.*, 1991). Overexpression of syndecan-1 in cultured NIH/3T3 or BHK fibroblasts and transfection of the syndecan-1 cDNA into the syndecan-1 deficient fusiform cells does not change their mesenchymal morphology to an epithelial one (Kato and Bernfield, unpublished results). No morphological change accompanies the increased syndecan-1 expression induced in NIH/3T3 fibroblasts by the combination of transforming growth factor-β and basic fibroblast growth factor (Elenius *et al.*, 1992) or by the antimicrobial peptide PR-39 (Gallo *et al.*, 1994). Yet, expression of syndecan-1 in transformed S115 cells and in Schwann cells does cause these cells to become rounder and more epithelial-like in shape (Leppä *et al.*, 1992; Carey *et al.*, 1994). Thus, overexpression of syndecan-1 in mesenchymal cells does not induce a transformation to epithelial cell morphology or organization.

Syndecan-1 Deficiency Correlates with Changes in the Expression of Other Adhesion Molecules

The change in cellular morphology and organization induced by syndecan-1 deficiency seen here are similar to those seen after the disruption of epithelial monolayers with antibodies directed against β1-integrins or E-cadherin (Yoshida-Noro *et al.*, 1984; Larjava *et al.*, 1990; Symington *et al.*, 1993). Both β1-integrins and E-cadherin localize at the lateral surfaces of the parental NMuMG cells, the vector-only transfectants, and the epithelial antisense transfectants in an identical manner as in other epithelial cells. These adhesion receptors are expressed differently in the fusiform antisense transfectants: the β1-integrins are now distributed over the entire cell surface (Figures 7 and 8), and E-cadherin expression is reduced to undetectable amounts at both the protein and mRNA level (Figures 9 and 10). Though disposed differently, the β1-integrins probably function because these cells adhere to and migrate on collagen gels (Figure 5), an activity that presumably involves β_1-integrins.

As in the current study, other epithelia modified to become fusiform in shape also lose E-cadherin expression and undergo a morphologic transformation. When murine epiblast cells are treated with anti-E–cadherin antibodies, the cells become fusiform, lose anchorage dependence for growth, drastically reduce E-cadherin expression, and maintain these changes despite removal of the antibody (Burdsal *et al.*, 1993). When mammary epithelia transfected with a c-*fos*–estradiol receptor fusion construct are treated with estradiol, c-*fos* is expressed, and the cells become fusiform, acquire the ability to invade collagen gels, and no longer express E-cadherin (Reichmann *et al.*, 1992). Moloney sarcoma virus-transformed MDCK cells that express low levels of E-cadheirn acquire a fibroblastic morphology and the ability to invade collagen gels (Behrens *et al.*, 1989). Overexpression of a functional erbB2 proto-oncogene in human mammary epithelial cells causes a marked reduction in E-cadherin transcription and loss of the ability to form three-dimensional structure in collagen gels (D'Souza *et al.*, 1993). In each of these instances, the transformed cells also acquire anchorage-independent growth. Thus, antibody treatment, oncogene expression, and syndecan-1 deficiency are distinct inciting events that cause epithelial cells to lose E-cadherin expression while acquiring mesenchyme-like morphology and behavior. The mechanism of this loss is unclear.

Basis for the Phenotypic Change Induced by Syndecan-1 Deficiency

Syndecan-1 is a transmembrane protein and thus can influence cellular behavior by either its extracellular or intracellular interactions. Extracellularly, via its heparan sulfate chains, syndecan-1 can anchor cells to the extracellular matrix (Koda *et al.*, 1985; Saunders and Bernfield, 1988; Sun *et al.*, 1989; Salmivirta *et al.*, 1991) and act as a coreceptor for basic fibroblast growth factor (Kiefer *et al.*, 1990; Bernfield and Hooper, 1991). Furthermore, cell surface heparan sulfate is a binding site for a variety of cytokines, degradative enzymes, and protease inhibitors (Bernfield *et al.*, 1992). Although its intracellular interactions are not as well defined, binding, co-localization, and detergent extraction studies suggest that syndecan-1 associates with the actin cytoskeleton (Rapraeger and Bernfield, 1982; Rapraeger *et al.*, 1986). Studies with heparin suggest that syndecan-1 does not maintain epithelial morphology and organization solely via the interactions of its heparan sulfate chains. Heparin at 10–25

μg/ml causes epithelia to lose their lobular or ductal morphology in organ culture or within collagen gels (Ekblom *et al.*, 1978; Bernfield *et al.*, 1984; Platt *et al.*, 1990). Yet, treatment of NMuMG cell monolayers with heparin at substantially higher concentrations has no effect on the morphology or organization of the cells (Bernfield, unpublished observation). Because exogenous heparin would compete with the heparan sulfate at the cell surface, the phenotypic changes induced by syndecan-1 deficiency are not likely due to lack of cell surface heparan sulfate.

The basis for the unique phenotype seen here is not entirely clear. But because E-cadherin is known to maintain the intercellular adhesions of epithelia, this epithelial to fusiform cell transformation correlates most with the loss of E-cadherin expression. This could account for the appearance of single cells that have lost epithelial shape, that under- and overlap adjacent cells, and that migrate into collagen gels (Figures 1 and 5). The change in actin filament organization (Figure 6) could be a consequence of the absence of the E-cadherin/catenin complex that mediates anchorage to adhesion junctions (Birchmeier *et al.*, 1993; Gumbiner and McCrea, 1993). Further, an epithelial-like morphology does not result when syndecan-1 is induced or overexpressed in mesenchymal cells (which lack E-cadherin), yet E-cadherin overexpression in such cells (which produce little cell surface syndecan-1) results in acquisition of an epithelial-like morphology (Nagafuchi *et al.*, 1987; McNeill *et al.*, 1990; Ozawa *et al.*, 1990). Thus, E-cadherin may be key to the maintenance of epithelial morphology by syndecan-1.

The basis for the anchorage-independent growth of the syndecan-deficient cells is also not clear. Syndecan-1 may be involved in organizing the E-cadherin/catenin complex in these cells into an adherens junction because each molecule is found at this site, and cells lacking these complexes show deranged growth control (Behrens *et al.*, 1989; Vleminckx *et al.*, 1991). Another possibility is that syndecan-1 has a role in delivering anchorage-dependent growth signals to the cell, and indeed, certain neoplastically transformed cells do have reduced levels of cell surface syndecan-1 (Leppä *et al.*, 1991; Inki *et al.*, 1994). If, as with other cells, this in vitro growth characteristic correlates with tumorigenicity, then the level of cell surface syndecan-1 may be a useful indicator of malignant potential.

Lack of E-cadherin expression and a loss of actin cytoskeletal organization appear to be the major molecular consequences of syndecan-1 deficiency in epithelia. How this effect is mediated is unclear because the intracellular interactions of syndecan-1 are not established. Moreover, the signaling pathways leading to changes in E-cadherin transcription and in actin organization are poorly understood. Syndecan-1 could interact intracellularly with a large variety of proteins, including membrane receptor tyrosine kinases, the panoply of proteins that organize, cross-link, or tether F-actin to the plasma membrane, or with the E-cadherin/catenin complex, e.g. at an adhesion junction. Alternatively, syndecan-1 could act indirectly through classical second messengers, protein kinases, or modification of membrane phospholipids.

ACKNOWLEDGMENTS

We thank Drs. R.L. Ceriani, R. Hynes, L. Kedes, E.B. Lane, and M. Takeichi, for providing precious reagents, and Olga Goldberger and Kevin Hooper for technical assistance. We also acknowledge an Arthritis Foundation Postdoctoral Fellowship for M.K., and National Institutes of Health grants (HD-0673, CA-28735, and HL-46491) for M.B.

REFERENCES

Amini, S., DeSeau, V., Reddy, S., Shalloway, D., and Bolen, J.B. (1986). Regulation of $pp60^{c\text{-}src}$ synthesis by inducible RNA complementary to c-src mRNA in polyomavirus-transformed rat cells. Mol. Cell. Biol. *6*, 2305–2316.

Behrens, J., Mareel, M.M., Van Roy, F.M., and Birchemier, W. (1989). Dissecting tumor cell invasion: epithelial cells acquire invasive properties after the loss of uvomorulin-mediated cell-cell adhesion. J. Cell Biol. *108*, 2435–2447.

Bernfield, M., Banerjee, S.D., Koda, J.E., and Rapraeger, A.C. (1984). Remodelling of the basement membrane: morphogenesis and maturation. In: Basement Membranes and Cell Movement (Ciba Foundation Symposium), ed. R. Porter and J. Whelan, London, UK: Pitman Publishing, 179–196.

Bernfield, M., and Hooper, K.C. (1991). Possible regulation of FGF activity by syndecan, an integral membrane heparan sulfate proteoglycan. Ann. NY Acad. Sci. *638*, 182–194.

Bernfield, M., Kokenyesi, R., Kato, M., Hinkes, M.T., Spring, J., Gallo, R.L., and Lose, E.J. (1992). Biology of syndecans: a family of transmembrane heparan sulfate proteoglycans. Annu. Rev. Cell Biol. *8*, 365–393.

Bernfield, M., Rapraeger, A., Jalkanen, M., and Banerjee, S.D. (1985). Matrix interactions in epithelial morphogenesis involve a cell surface proteoglycan. In: Basement Membranes, ed. S. Shibata, Amsterdam, The Netherlands: Elsevier, 343–352.

Birchmeier, W., Weidner, K.M., and Beherens, J. (1993). Molecular mechanisms leading to loss of differentiation and gain of invasiveness in epithelial cells. J. Cell Sci. Suppl. *17*, 159–164.

Burdsal, C.A., Damsky, C.H., and Pedersen, R.A. (1993). The role of E-cadherin and integrins in mesoderm differentiation and migration at the mammalian primitive streak. Development *118*, 829–844.

Carey, D.J., Stahl, R.C., Cizmeci-Smith, G., and Asundi, V.K. (1994). Syndecan-1 expressed in Schwann cells causes morphological transformation and cytoskeletal reorganization and associates with actin during cell spreading. J. Cell Biol. *124*, 161–170.

Ceriani, R.L., and Peterson, J.A. (1978). Characterization of differentiation antigens of the mouse mammary epithelial cell (MME antigens) carried on the mouse milk fat globule. Cell Differ. *7*, 355–366.

D'Souza, B., Berdichevsky, F., Kyprianou, N., and Taylor-Papadimitriou, J. (1993). Collagen-induced morphogenesis and expression of the α2-integrin subunit is inhibited in c-erbB2–transfected human mammary epithelial cells. Oncogene *8*, 1797–1806.

David, G., and Bernfield, M. (1979). Collagen reduces glycosaminoglycan degradation by cultured mammary epithelial cells: possible mechanism for basal lamina formation. Proc. Natl. Acad. Sci. USA *76*, 786–790.

David, G., Van der Schueren, B., and Bernfield, M. (1981). Basal lamina formation by normal and transformed mouse mammary epithelial cells duplicated in vitro. J. Natl. Cancer Inst. *67*, 719–728.

Ekblom, P., Nordling, S., and Saxén, L. (1978). Inhibition of kidney tubule induction by charged polymers. Cell Differ. *7*, 345–353.

Elenius, K., Määttä, A., Salmivirta, M., and Jalkanen, M. (1992). Growth factors induce 3T3 cells to express bFGF-binding syndecan. J. Biol. Chem. *267*, 6435–6441.

Elenius, K., Vainio, S., Laato, M., Salmivirta, M., Thesleff, I., and Jalkanen, M. (1991). Induced expression of syndecan in healing wounds. J. Cell Biol. *114*, 585–595.

Estival, A., Louvel, D., Couderc, B., Prats, H., Hollande, E., Vaysse, N., and Clémente, F. (1993). Morphological and biological modifications induced in a rat pancreatic acinar cancer cell line (AR4–2J) by unscheduled expression of basic fibroblast growth factors. Cancer Res. *53*, 1182–1187.

Fitchett, J.E., and Hay, E.D. (1989). Medial edge epithelium transforms to mesenchyme after embryonic palatal shelves fuse. Dev. Biol. *131*, 455–474.

Gallo, R.L., Ono, M., Povsic, T., Page, C., Eriksson, E., Klagsbrun, M., and Bernfield, M. (1994). Syndecans, cell surface heparan sulfate proteoglycans, are induced by a proline-rich antimicrobial peptide from wounds. Proc. Natl. Acad. Sci. USA *91*, 11035-11039.

Gherardi, E., Gray, J., Stoker, M., Perryman, M., and Furlong, R. (1989). Purification of scatter factor, a fibroblast-derived basic protein that modulates epithelial interactions and movement. Proc. Natl. Acad. Sci. USA *86*, 5844–5848.

Godson, C., Bell, K.S., and Insel, P.A. (1993). Inhibition of expression of protein kinase Cα by antisense cDNA inhibits phorbol ester-mediated arachidonate release. J. Biol. Chem. *268*, 11946-11950.

Greenburg, G., and Hay, E.D. (1986). Cytodifferentiation and tissue phenotype change during transformation of embryonic lens epithelium to mesenchyme-like cells in vitro. Dev. Biol. *115*, 363–379.

Greenburg, G., and Hay, E.D. (1988). Cytoskeleton and thyroglobulin expression change during transformation of thyroid epithelium to mesenchyme-like cells. Development *102*, 605–622.

Gumbiner, B.M., and McCrea, P.D. (1993). Catenins as mediators of the cytoplasmic functions of cadherins. J. Cell Sci. Suppl. *17*, 155–158.

Gunning, P., Leavitt, J., Muscat, G., Ng, S.-Y., and Kedes, L. (1987). A human β-actin expression vector system directs high-level accumulation of antisense transcripts. Proc. Natl. Acad. Sci. USA *84*, 4831–4835.

Hall, H.G., Farson, D.A., and Bissell, M.J. (1982). Lumen formation by epithelial cell lines in response to collagen overlay: a morphogenetic model in culture. Proc. Natl. Acad. Sci. USA *79*, 4672–4676.

Hay, E.D. (1991). Collagen and other matrix glycoproteins in embryogenesis. In: Cell Biology of Extracellular Matrix, ed. E.D. Hay, New York: Plenum, 419–462.

Hayashi, K., Hayashi, M., Jalkanen, M., Firestone, J.H., Trelstad, R.L., and Bernfield, M. (1987). Immunocytochemistry of cell surface heparan sulfate proteoglycan in mouse tissues: a light and electron microscopic study. J. Histochem. Cytochem. *35*, 1079–1088.

Hirai, Y., Nose, A., Kobayash, S., and Takeichi, M. (1989). Expression and role of E- and P-cadherin adhesion molecules in embryonic histogenesis. I. Lung epithelial morphogenesis. Development *105*, 263–270.

Hynes, R.O., and Destree, A.T. (1978). 10 nm filaments in normal and transformed cells. Cell *13*, 151–163.

Hynes, R.O., Marcantonio, E.E., Stepp, M.A., Urry, L.A., and Yee, G.H. (1989). Integrin heterodimer and receptor complexity in avian and mammalian cells. J. Cell Biol. *109*, 409–420.

Inki, P., Larjava, H., Haapasalmi, K., Miettinen, H.M., Grenman, R., and Jalkanen, M. (1994). Expression of syndecan-1 is induced by differentiation and suppressed by malignant transformation of human keratinocytes. Eur. J. Cell Biol. *63*, 43–51.

Jalkanen, M., Nguyen, H., Rapraeger, A., Kurn, N., and Bernfield, M. (1985). Heparan sulfate proteoglycans from mouse mammary epithelial cells: localization on the cell surface with a monoclonal antibody. J. Cell Biol. *101*, 976–984.

Jalkanen, M., Rapraeger, A., Saunders, S., and Bernfield, M. (1987). Cell surface proteoglycan of mouse mammary epithelial cells is shed by cleavage of its matrix-binding ectodomain from its membrane-associated domain. J. Cell Biol. *105*, 3087–3096.

Jue, S.F., Bradley, R.S., Rudnicki, J.A., Varmus, H.E., and Brown, A.M.C. (1992). The mouse wnt-1 gene can act via a paracrine mechanism in transformation of mammary epithelial cells. Mol. Cell. Biol. *12*, 321–328.

Kiefer, M.C., Stephans, J.C., Crawford, K., Okino, K., and Barr, P.J. (1990). Ligand-affinity cloning and structure of a cell surface heparan sulfate proteoglycan that binds basic fibroblast growth factor. Proc. Natl. Acad. Sci. USA *87*, 6985–6989.

Kim, C.W., Goldberger, O.A., Gallo, R.L., and Bernfield, M. (1994). Members of the syndecan family of heparan sulfate proteoglycans are expressed in distinct cell-, tissue-, and development-specific patterns. Mol. Biol. Cell *5*, 797–805.

Koda, J., and Bernfield, M. (1984). Heparan sulfate proteoglycans from mouse mammary epithelial cells: basal extracellular proteoglycan binds specifically to native type I collagen fibrils. J. Biol. Chem. *259*, 11763-11770.

Koda, J.E., Rapraeger, A., and Bernfield, M. (1985). Heparan sulfate proteoglycans from mouse mammary epithelial cells: cell surface proteoglycan as a receptor for interstitial collagens. J. Biol. Chem. *260*, 8157–8162.

Kokenyesi, R., and Bernfield, M. (1994). Core protein structure and sequence determine the site and presence of heparan sulfate and chondroitin sulfate on syndecan-1. J. Biol. Chem. *269*, 12304-12309.

Laemmli, U.K. (1970). Cleavage of structural proteins during the assembly of the head of bacteriophage T4. Nature *227*, 680–685.

Lane, E.B. (1982). Monoclonal antibodies provide specific intramolecular markers for the study of epithelial tonofilament organization. J. Cell Biol. *92*, 665–673.

Larjava, H., Peltonen, J., Akiyama, S.K., Yamada, S.S., Gralnick, H.R., Uitto, J., and Yamada, K.M. (1990). Novel function for β1 integrins in keratinocyte cell-cell interaction. J. Cell Biol. *110*, 803–815.

Leppä, S., Härkönen, P., and Jalkanen, M. (1991). Steroid-induced epithelial-fibroblastic conversion associated with syndecan suppression in S115 mouse mammary tumor cells. Cell Regul. *2*, 1–11.

Leppä, S., Mali, M., Miettinen, H.M., and Jalkanen, M. (1992). Syndecan expression regulates cell morphology and growth of mouse mammary epithelial tumor cells. Proc. Natl. Acad. Sci. USA *89*, 932–936.

Lories, V., Cassiman, J.-J., Van den Berghe, H., and David, G. (1992). Differential expression of cell surface heparan sulfate proteoglycans in human mammary epithelial cells and lung fibroblasts. J. Biol. Chem. *267*, 1116–1122.

Marcantonio, E.E., and Hynes, R.O. (1988). Antibodies to the conserved cytoplasmic domain of the integrin β1 subunit react with

proteins in vertebrates, invertebrates, and fungi. J. Cell Biol. *106*, 1765–1772.

McAlmon, K.R. (1992). Matrix receptors and development. Semin. Perinatol. *16*, 90–96.

McNeill, H., Ozawa, M., Kemler, R., and Nelson, W.J. (1990). Novel function of the cell adhesion molecule uvomorulin as an inducer of cell surface polarity. Cell *62*, 309–316.

Morrison, M. (1974). The determination of the exposed proteins on membranes by the use of lactoperoxidase. Methods Enzymol. *32*, 103–109.

Nagafuchi, A., Shirayoshi, Y., Okazaki, K., Yasuda, K., and Takeichi, M. (1987). Transformation of cell adhesion properties by exogenously introduced E-cadherin cDNA. Nature *329*, 341–343.

Oettinger, H.F., Streeter, H., Lose, E., Copeland, N.G., Gilbert, D.J., Justice, M.J., Jenkins, N.A., Mohandas, T., and Bernfield, M. (1991). Chromosome mapping of the murine syndecan gene. Genomics *11*, 334–338.

Owens, R.B., Smith, H.S., and Hackett, A.J. (1974). Epithelial cell cultures from normal glandular tissue of mouse. J. Natl. Cancer Inst. *53*, 261–269.

Ozawa, M., Ringwald, M., and Kemler, R. (1990). Uvomorulin-catenin complex formation is regulated by a specific domain in the cytoplasmic region of the cell adhesion molecule. Proc. Natl. Acad. Sci. USA *87*, 4246–4250.

Platt, J.L., Trescony, P., Lindman, B., and Oegema, T.R. (1990). Heparin and heparan sulfate delimit nephron formation in fetal metanephric kidneys. Dev. Biol. *139*, 338–348.

Rapraeger, A., Jalkanen, M., and Bernfield, M. (1986). Cell surface proteoglycan associates with the cytoskeleton at the basolateral cell surface of mouse mammary epithelial cells. J. Cell Biol. *103*, 2683–2696.

Rapraeger, A.C., and Bernfield, M. (1982). An integral membrane proteolgycan is capable of binding components of the cytoskeleton and the extracellular matrix. In: Extracellular Matrix, ed. S. Hawkes and J.L. Wang, New York: Academic Press, 265–269.

Reichmann, E., Schwarz, H., Deiner, E.M., Leitner, I., Eilers, M., Berger, J., Busslinger, M., and Beug, H. (1992). Activation of an inducible c-Fos ER fusion protein causes loss of epithelial polarity and triggers epithelial-fibroblastoid cell conversion. Cell *71*, 1103–1116.

Salmivirta, M., Elenius, K., Vainio, S., Hofer, U., Chiquet-Ehrismann, R., Thesleff, I., and Jalkanen, M. (1991). Syndecan from embryonic tooth mesenchyme binds tenascin. J. Biol. Chem. *266*, 7733–7739.

Sambrook, J., Fritsch, E.F., and Maniatis, T. (1989). Molecular Cloning: A Laboratory Manual, Cold Spring Harbor, NY: Cold Spring Harbor Laboratory Press.

Sanderson, R.D., Hinkes, M.T., and Bernfield, M. (1992). Syndecan-1, a cell-surface proteoglycan, changes in size and abundance when keratinocytes stratify. J. Invest. Dermatol. *99*, 390–396.

Saunders, S., and Bernfield, M. (1988). Cell surface proteoglycan binds mouse mammary epithelial cells to fibronectin and behaves as a receptor for interstitial matrix. J. Cell Biol. *106*, 423–430.

Saunders, S., Jalkanen, M., O'Farrell, S., and Bernfield, M. (1989). Molecular cloning of syndecan, an integral membrane proteoglycan. J. Cell Biol. *108*, 1547–1556.

Shirayoshi, Y., Nose, A., Iwasaki, K., and Takeichi, M. (1986). *N*-linked oligosaccharides are not involved in the function of a cell-cell binding glycoprotein E-cadherin. Cell Struct. Funct. *11*, 245–252.

Solursh, M., Reiter, R.S., Jensen, K.L., Kato, M., and Bernfield, M. (1990). Transient expression of a cell surface heparan sulfate proteoglycan (syndecan) during limb development. Dev. Biol. *140*, 83–92.

Sun, X., Mosher, D.F., and Rapraeger, A. (1989). Heparan sulfate-mediated binding of epithelial cell surface proteoglycan to thrombospondin. J. Biol. Chem. *264*, 2885–2889.

Sutherland, A.E., Sanderson, R.D., Mayes, M., Seibert, M., Calarco, P.G., Bernfield, M., and Damsky, C.H. (1991). Expression of syndecan, a putative low affinity fibroblast growth factor receptor, in the early mouse embryo. Development *113*, 339–351.

Symington, B.E., Takada, Y., and Carter, W.G. (1993). Interaction of integrins $\alpha 3\beta 1$ and $\alpha 2\beta 1$: potential role in keratinocyte intercellular adhesion. J. Cell Biol. *120*, 523–535.

Takeichi, M. (1988). The cadherins: cell-cell adhesion molecules controlling animal morphogenesis. Development *102*, 639–655.

Thesleff, I., Jalkanen, M., Vainio, S., and Bernfield, M. (1988). Cell surface proteoglycan expression correlates with epithelial-mesenchymal interaction during tooth morphogenesis. Dev. Biol. *129*, 565–572.

Trautman, M.S., Kimelman, J., and Bernfield, M. (1991). Developmental expression of syndecan, an integral membrane proteoglycan, correlates with cell differentiation. Development *111*, 213–220.

Vallés, A.M., Tucker, G.C., Thiery, J.P., and Boyer, B. (1990). Alternative patterns of mitogenesis and cell scattering induced by acidic FGF as a function of cell density in a rat bladder carcinoma cell line. Cell Regul. *1*, 975–988.

Vleminckx, K., Vakaet, L., Jr., Mareel, M., Fiers, W., and Van Roy, F. (1991). Genetic manipulation of E-cadherin expression by epithelial tumor cells reveals an invasion suppressor role. Cell *66*, 107–119.

Weidner, K.M., Behrens, J., Vandekerckhove, J., and Birchmeier, W. (1990). Scatter factor: molecular characteristics and effect on the invasiveness of epithelial cells. J. Cell Biol. *111*, 2097–2108.

Wenz, H.-M., Hinck, L., Cannon, P., Navre, M., and Ringold, G.M. (1992). Reduced expression of AP27 protein, the product of a growth factor-repressible gene, is associated with diminished adipocyte differentiation. Proc. Natl. Acad. Sci. USA *89*, 1065–1069.

Yoshida-Noro, C., Suzuki, N., and Takeichi, M. (1984). Molecular nature of the calcium-dependent cell-cell adhesion system in mouse teratocarcinoma and embryonic cells studied with a monoclonal antibody. Dev. Biol. *101*, 19–27.

Zuk, A., Matlin, K.S., and Hay, E.D. (1989). Type I collagen gel induces Madin-Darby canine kidney cells to become fusiform in shape and lose apical-basal polarity. J. Cell Biol. *108*, 903–919.